

GA-A22865

**EFFECTS OF PARTICLE EXHAUST ON NEUTRAL
COMPRESSION RATIOS IN DIII-D**

by
**R.J. COLCHIN, R. MAINGI, S.L. ALLEN, C.M. GREENFIELD,
and M.R. WADE**

AUGUST 1998

DISCLAIMER

This report was prepared as an account of work sponsored by an agency of the United States Government. Neither the United States Government nor any agency thereof, nor any of their employees, makes any warranty, express or implied, or assumes any legal liability or responsibility for the accuracy, completeness, or usefulness of any information, apparatus, product, or process disclosed, or represents that its use would not infringe privately owned rights. Reference herein to any specific commercial product, process, or service by trade name, trademark, manufacturer, or otherwise, does not necessarily constitute or imply its endorsement, recommendation, or favoring by the United States Government or any agency thereof. The views and opinions of authors expressed herein do not necessarily state or reflect those of the United States Government or any agency thereof.

EFFECTS OF PARTICLE EXHAUST ON NEUTRAL COMPRESSION RATIOS IN DIII-D

by
R.J. COLCHIN,[†] R. MAINGI,[†] S.L. ALLEN,[‡] C.M. GREENFIELD,
and M.R. WADE[†]

This is a preprint of a paper to be presented at the 13th International Conference on Plasma Surface Interactions on Controlled Fusion Devices, May 18–23, 1998, San Diego, California and to be published in *Journal of Nuclear Materials*.

[†]Oak Ridge National Laboratory
[‡]Lawrence Livermore National Laboratory

Work supported by
the U.S. Department of Energy
under Contracts DE-AC03-89ER51114, DE-AC05-96OR22464,
and W-7405-ENG-48

GA PROJECT 3466
AUGUST 1998

ABSTRACT

In this paper, neutral particles in DIII-D are studied via their compression in the plenum and via particle exhaust. The compression of gas in the plenum is examined in terms of the magnetic field configuration and wall conditions. DIII-D compression ratios are observed in the range from 1 to ≥ 1000 . Particle control ultimately depends on the exhaust of neutrals via plenum or wall pumping. Wall pumping or outgassing is calculated by means of a detailed particle balance throughout individual discharges, and its effect on particle control is discussed. It is demonstrated that particle control through wall conditioning leads to lower normalized densities. A two-region model shows that the gas compression ratio (C_{div} = divertor plenum neutral pressure/torus neutral pressure) can be interpreted in relation to gas flows in the torus and divertor including the pumping speed of the plenum cryopumps, plasma pumping, and the pumping or outgassing of the walls.

1. INTRODUCTION

Tokamaks and internal combustion engines are similar in that they both take in gas, heat it to high temperatures and pressures, and subsequently exhaust the hot gasses. In a tokamak, the divertor acts as the exhaust manifold, and its efficiency is key to tokamak particle control.

An efficient divertor is one in which fuel particles that leave the plasma are locally isolated and neutralized in a manner that allows for dissipation of their heat and also their removal from the vessel. An important subsidiary condition is that minimal impurities flow from the divertor region back into the plasma. Enormous progress has been made in recent years in understanding and creating efficient divertors [1]. A measure of this progress is the degree to which the divertors isolate the neutrals flowing out of the plasma. A factor characterizing this isolation is the ratio of the divertor to the torus plenum pressures called the neutral compression factor, C_{div} [2–3]. The compression factor can be related to other neutrals flows (see Section 5).

Particle control depends on particle exhaust via divertor and wall pumping. Wall equilibration times in existing tokamaks are of the same magnitude or longer than discharge times, and so can act as sources or sinks for neutral particles. This is particularly true of tokamaks such as DIII-D which have carbon wall tiles and practice extensive wall conditioning. Wall pumping (outgassing) changes with time during discharges can be calculated by use of a global gas balance [4–6]

$$Q_{wall} \equiv Q_{wall}^S + Q_{wall}^D = [Q_{ext}^D + Q_{ext}^S] - \left[Q_{cryo} + \frac{dN_i}{dt} + \frac{dN_0}{dt} \right] \quad (1)$$

where the S superscript represents the main chamber scrape-off layer (SOL) and the D superscript represents the divertor. The Q_{ext} and Q_{cryo} terms represent external gas inputs and divertor cryopump outputs (Torr-l/s). The terms dN_i/dt and dN_0/dt are the rates of change of the plasma and plenum particle and gas inventories, respectively. These terms are usually small during the steady-state portion of the pulse, and are calculated by assuming $N_i = N_e$. The sign convention is such that $Q_{wall} > 0$ implies a pumping wall. This convention is used throughout the paper for the wall term, and the gas flows are expressed in Torr-l/s, with one Torr-l equal to $\sim 7 \times 10^{19}$ atoms. It is informative to compare Q_{wall} with the divertor exhaust rate Q_{cryo} to determine the mechanism responsible for particle exhaust. If Q_{wall} is negative (wall outgassing) and larger than Q_{cryo} , increasing plasma density can lead to discharge termination.

Section 2 gives a brief discussion of the experimental arrangement of pumps and diagnostics. Section 3 gives the results of DIII-D measurements, Section 4 presents the results of wall conditioning on density limits, Section 5 discusses the compression ratio, and Section 6 summarizes the results.

2. EXPERIMENTAL ARRANGEMENT AND DIAGNOSTICS

DIII-D has both upper and lower divertors, which have associated pumping chambers (plena) and cryopumps with pumping speeds of ~ 35 kl/s at 10^{-3} Torr plenum pressure. Pump locations are shown in Fig. 1. The lower divertor is not tightly baffled (open divertor) while the upper divertor is more tightly baffled (closed divertor) [7,8]. The torus is pumped by turbopumps with a pumping speed of 7.5 kl/s. The pumping speed of the plasma is much larger, and so the effect of the turbopumps on the neutral population can be neglected during a discharge.

There are fast-time-response ($\tau \sim 1$ ms) ionization gauges located in the upper and lower divertor plena [9,10] and on the torus midplane (Fig. 1). These gauges are shielded to eliminate the effects of direct bombardment by plasma particles and ultraviolet light. The gauge sensitivities are calibrated *in situ* (as a function of pressure and magnetic field) in relation to magnetically shielded MKS capacitance manometers¹ located in the torus and the upper divertor plenum.

Data for the calculation of the particle balance are obtained from calibrated gas valves, interferometer data for the plasma density, and neutral beam power which gives the beam fueling rate [Q_{NBI} (Torr-l/s) $\cong 2.2 \times P_{NBI}$ (MW)].

The walls of the divertor chamber are constructed of carbon tiles. In DIII-D, only the outer legs of the separatrix are pumped, and the inner legs are exhausted back into the divertor plasma. Access to the plena is restricted at the throat, as shown in Fig. 1. The plenum throat apertures are toroidally symmetric and have vertical heights of 2.7 cm and 3.9 cm for the lower and upper plena, respectively. Measurements [7] made by moving the strike point of the outer separatrix leg relative to the plenum throats show that the divertor plenum pressures can be varied by factors of ~ 3 to 7. There are usually several minutes of helium glow discharge cleaning between tokamak discharges [11].

¹MKS Instruments Inc., Andover, Massachusetts.

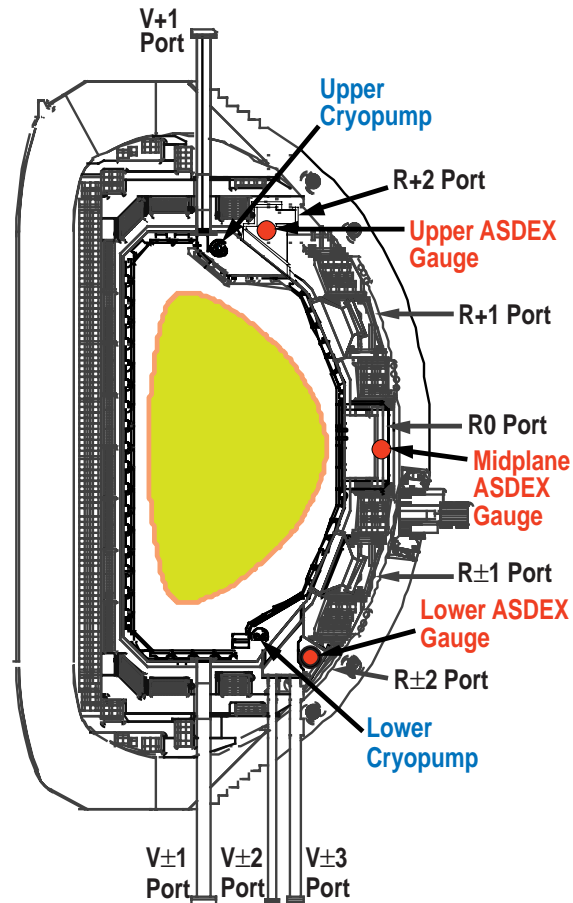


Fig. 1. Cross-sectional drawing of DIII-D showing the positions of the cryopumps in the upper and lower plena and the locations of the fast ionization (ASDEX) gauges.

3. MEASUREMENTS OF NEUTRAL PARTICLE COMPRESSION RATIOS AND PUMPING IN DIII-D

Typical compression ratios in diverted H-mode discharges are shown in Fig. 2. During divertor operation, pressures in the divertor plena are typically a maximum of a few milli-Torr and pressures at the torus midplane vary from a few times 10^{-5} Torr down to the low 10^{-7} Torr range. In “puff-and-pump” [12,13] discharges, Fig. 2(a), neutrals are introduced and ionized in the upper divertor and allowed to flow (as ions) along the separatrix into the opposite divertor, entraining impurities in the flow. After 1.3 s, this discharge enters the ELMing H-mode regime and the compression ratio is ~ 150 .

The highest compression ratios are found in low-density, ECH discharges. The middle trace of Fig. 2 shows that compression ratio can reach values larger than 1000. This is mainly due to the low pressure at the torus midplane ($<10^{-6}$ Torr). Two large ELMs occur around 2.2 s which result in noise spikes on the torus pressure gauge and cause the compression ratio to go off scale.

By changing the magnetic configuration during a discharge, it is possible to move from an inner-wall-limited non-divertor discharge to an upper-single-null diverted discharge. The results are shown in the lower traces of Fig. 2. The magnetic configuration is inner-wall-limited until 2.5 s, whereafter it is changed to upper-single-null. In the initial inner-wall-limited phase the compression is near one. There is a large transient at 2.5 s as the configuration is changed, whereafter the compression ratio is around 100.

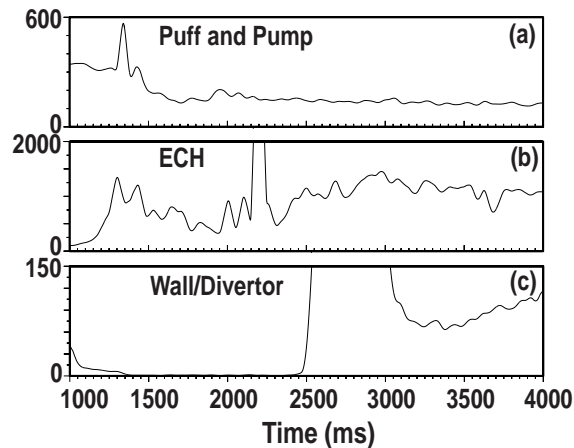


Fig. 2. Compression ratios (ratio of the divertor plenum pressure to the torus midplane pressure) in diverted ELMing DIII-D H-mode discharges. The top curve (a) is for “puff and pump” discharges in which gas is introduced in the upper divertor region and exhausted in the opposite (lower single-null) divertor. The middle curve (b) is for a low density, lower-single-null divertor discharge ($n_e < 10^{19} \text{ m}^{-3}$) heated by ECH and neutral beam injection. The lower curve (c) is for a discharge that was non-diverted up to 2500 ms and then moved to an upper-single-null diverted discharge whereupon it transitioned to the H-mode.

The wall pumping rates and inventories for the discharges shown in Fig. 2 are plotted in Fig. 3. During “puff and pump” discharges (top traces of Fig. 3), the wall acts as a sink of neutrals during the first half of this discharge, but half way through the discharge it transitions to negative values and acts as a net particle source. The net neutral inventory at the end of the discharge is zero. For the ECH discharge (middle traces of Fig. 3) the walls pump during feedback-controlled gas injection, as indicated by positive excursions in the wall gas flow rate. There is a net accumulation of neutrals in the walls throughout this discharge. The lower solid trace in Fig. 3 shows that the walls are a net sink of particles in the inner-wall-limited phase and a net source in the divertor phase. By the end of the discharge the net change in wall inventory is slightly negative.

In relation to particle exhaust control, the balance between wall and cryopump gas flows is shown in Fig. 4, which plots the ratio Q_{wall}/Q_{plena} for the discharges of Figs. 2 and 3. Cryopump flows dominate if the data lie in the shaded regions (i.e. within the ± 1 bands). For ratios greater than one, wall pumping gas flows are larger than flows to the cryopumps, and for ratios less than one, wall outgassing dominates. Using the previous convention, positive values indicate wall pumping and negative values indicate wall outgassing. During the initial phase of all three discharges wall pumping is largest, but later in the discharges the data have more of a tendency to lie within the ± 1 band limits of cryopump-dominated flow, indicating that particle exhaust is controlled.

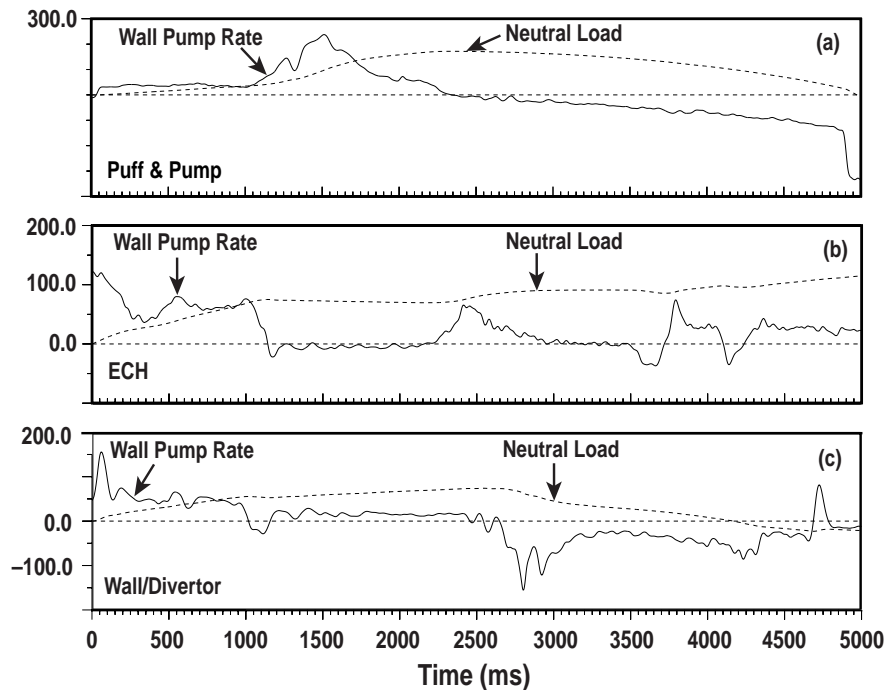


Fig. 3. Comparison of the wall source rates (solid curves – Torr-l/s) and the gas inventory (dashed curves – integral of the wall source rates – Torr-l) for the three discharges shown in Fig. 2.

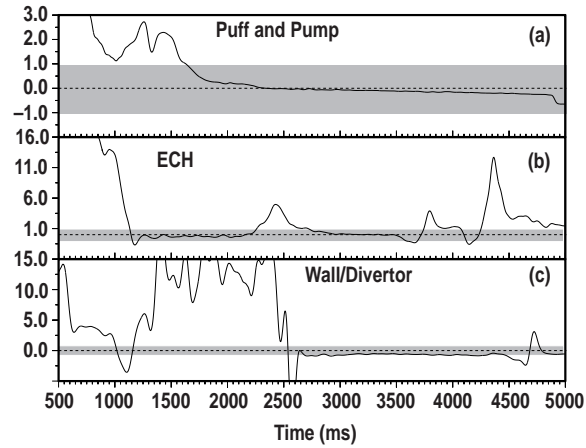


Fig. 4. Ratio of $Q_{\text{wall}}/Q_{\text{plasma}}$ for the three discharges shown in Figs. 2 and 3. For data lying within the shaded bands of ± 1 , flows to the cryopumps are larger than flows to the walls. For data outside the ± 1 bands, the opposite is true. Positive data values indicate that the wall is a net particle sink and negative values indicate that the wall is a net particle source.

4. PARTICLE CONTROL THROUGH WALL CONDITIONING

The attainment of quasi-steady-state advanced tokamak modes requires [14] control of the particle density so as to reach lower values of the plasma density ($n_e/n_{\text{Greenwald}}$). Current drive experiments also require low density plasmas. This in turn requires that wall outgassing be controlled. Figure 5 shows the minimum ratio of $n_e/n_{\text{Greenwald}}$ as a function of the net change in the wall inventory at the end of each discharge [computed by integrating Q_{wall}] for a number of H-mode and L-mode discharges. Here $n_{\text{Greenwald}}$ is given by Greenwald density limit scaling [15] and is a useful reference point when comparing discharges with different plasma currents and shapes. Each symbol type represents discharges which occurred on the same run day. The arrows indicate the trend of the net change in wall inventory after each discharge during the course of each day. Figure 5 shows that as each run day progressed, discharges moved in the direction of the positive x-axis, i.e., “strongly” outgassing discharges evolved to “weakly” outgassing discharges and “weakly” pumping discharges evolved to “strongly” pumping discharges. The absolute location of the zero point for each run day is uncertain because of the subtraction of large quantities in Eq. (1). However, the relative trend on each run day is clear. Thus, during each day’s run the walls become better conditioned and tend more toward acting as a getter. The group of H-mode points for which the wall is well conditioned and acts as a pump reaches the lowest values of $n_e/n_{\text{Greenwald}}$. This observation underscores the point that the walls must be strongly pumping to achieve the lowest $n_e/n_{\text{Greenwald}} \sim 0.27$ for the upper-single-null discharges. In comparison, the lowest $n_e/n_{\text{Greenwald}} \sim 0.22$ in lower-single-null discharges also occurred after extensive wall conditioning with the divertor cryopump [4]. The L-mode points have the lowest $n_e/n_{\text{Greenwald}}$ due to lower values of the particle confinement time, τ_p .

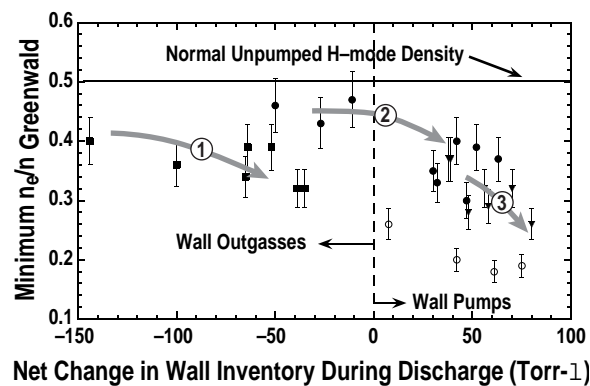
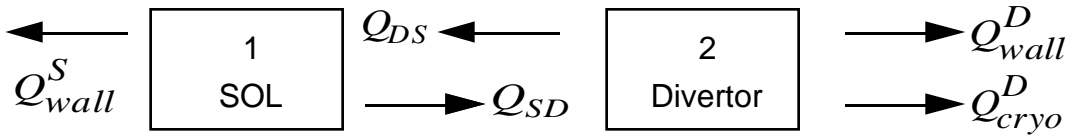


Fig. 5. Minimum value of $n_e/n_{\text{Greenwald}}$ versus the net change in wall inventory (Q_{wall}). Open circles indicate L-mode discharges with lower values of τ_p . Arrows indicate progression of data points during a day’s run.

5. DISCUSSION OF THE COMPRESSION RATIO

The compression ratio C_{div} is easily experimentally determined and is generally considered to be a measure of the effectiveness of a divertor. However the discussion below shows that it depends on a number of quantities some of which are not measured, which cloud the interpretation. The neutral compression ratio depends not only how efficiently the divertor screens neutrals from the main chamber, but also on the wall conditions. To assess this relationship, a two-region flow model is adopted with neutral flows as indicated schematically in the diagram below.



The neutral particle balance equations are:

$$dN_o^S / dt = S_{rec}^S + Q_{DS} - Q_{SD} - Q_{wall}^S - n_e^S P_o^D \langle \sigma v \rangle_{eii}^S V^S / T_o^S \quad (2)$$

$$dN_o^D / dt = S_{rec}^D + Q_{SD} - Q_{DS} - Q_{wall}^D - n_e^D P_o^D \langle \sigma v \rangle_{eii}^D V^D / T_o^D - Q_{cryo}. \quad (3)$$

In these relations, external gas inputs and ion-electron recombination are neglected for simplicity. The S_{rec} terms represent source terms for neutral particles, i.e. recycling of the plasma flux at material boundaries. The Q_{SD} and Q_{DS} terms represent neutral transport between the two chambers, the Q_{wall} terms represent pumping of neutrals at the material boundaries and the $n_e P_o \langle \sigma v \rangle_{eii} V / T_o$ terms represent electron impact ionization of neutrals in each chamber, where n_e is the electron density, P_o is the neutral pressure, $\langle \sigma v \rangle_{eii}$ is the electron impact ionization rate, V is the chamber volume, and T_o is the neutral temperature. There is an additional loss term in the divertor due to neutrals which are exhausted by the cryopump, $Q_{cryo} = S_{cryo} P_{plenum}$ where S_{cryo} is the pumping speed and P_{plenum} is the plenum neutral pressure.

By substituting for Q_{cryo} , assuming steady-state, recognizing that $Q_{DS} \gg Q_{SD}$ (neutrals leak out of the divertor to the main chamber), rearranging terms in the equations and dividing Eq. (3) by Eq. (2), the following relation is derived for the neutral compression ratio:

$$C_{div} \equiv \frac{P_{plenum}^S}{P_o^S} = \frac{(S_{rec}^D - Q_{DS} - Q_{wall}^D - n_e^D P_o^D \langle \sigma v \rangle_{eii}^D V^D / T_o^D)}{(S_{rec}^S + Q_{DS} - Q_{wall}^S)} \cdot \frac{T_o^S}{n_e^S \langle \sigma v \rangle_{eii}^S V^S S_{cryo}}. \quad (4)$$

There is direct evidence for the inverse dependence of C_{div} on S_{cryo} . When the cryopumps were warmed between DIII-D H-mode discharges, C_{div} increased by a factor of two.

One goal of a divertor is to minimize Q_{DS} . In the limit of a “good” divertor design, $Q_{DS} < Q_{cryo}$ and can be neglected in the numerator of Eq. (4). Also if “pumping” wall conditions are assumed in the main chamber, $S_{rec}^S \approx Q_{wall}^S$, then Q_{DS} is the dominant term in the denominator of Eq. (4). For these idealized conditions, $C_{div} \sim 1/Q_{DS}$, i.e. improving divertor efficiency by reducing Q_{DS} yields a linear increase in C_{div} . This can explain the increased values of the compression ratio observed during ECH discharges. Equation (4) shows the danger in interpreting C_{div} as a measure of Q_{DS} : a change in C_{div} could be caused by a change in the wall pumping state in the divertor, Q_{wall}^D . Practically one must consider recycling in the main chamber also as it is difficult to determine conditions for the validity of $Q_{DS} > (S_{rec}^S - Q_{wall}^S)$.

6. SUMMARY

Neutral particles are studied in DIII-D in relation to the compression ratio and particle control. A survey of DIII-D compression ratios reveals a range from ≥ 1000 for low-density diverted plasmas to approximately one for inner-wall-limited plasmas. Typical compression ratios for ELMing “puff and pump” experiments are ~ 150 , while normal ELMing H-mode plasmas have compressions of ~ 30 – 100 . L-mode compressions are usually higher. Measurements also show the walls switching between being neutral gas sinks and neutral gas sources during a discharge, an effect that is important for particle control.

With good wall conditioning, improved particle control can be achieved as indicated by lower values of $n_e/n_{\text{Greenwald}}$. To date the lowest $n_e/n_{\text{Greenwald}} \sim 0.27$ in optimized upper-single null discharges, compared with $n_e/n_{\text{Greenwald}} \sim 0.22$ in optimized lower-single null discharges.

DIII-D compression ratio measurements can be qualitatively compared with previously reported results from Alcator C-Mod [3]. Divertor and midplane neutral pressures in Alcator are typically 10 to 100 times those in DIII-D. Compression ratios in Alcator were limited to ~ 70 by particle leakage out of the divertor plenum, but were later increased to above 100 when the plenum leaks were closed. Compression ratios tend lower with lower densities in Alcator C-Mod [3,16], whereas the highest compression ratios have been observed at the lowest densities in DIII-D.

REFERENCES

- [1] See articles in the Proceedings of the Twelfth International Conference on Plasma-Surface Interactions, (May 20-24, 1996, Saint-Raphaël, France) *J. Nucl. Mater.* **241-243** (1997).
- [2] H.F. Dylla, *et al.*, *J. Nucl. Mater.* **121** (1984) 144.
- [3] A. Niemczewski, I.H. Hutchinson, B. LaBombard, B. Lipschultz, and G.M. McCracken, *Nucl. Fusion* **37** (1997) 151.
- [4] R. Maingi *et al.*, *Nucl. Fusion* **36** (1996) 245.
- [5] R. Maingi *et al.*, *J. Nucl. Mater.* **241-243** (1997) 672.
- [6] M.A. Madavi *et al.*, in *Controlled Fusion and Plasma Physics* (Proc. 20th European Conf. Lisbon, 1993) Vol. 17C, Part II, (European Physical Society, Geneva), 1993, p. 647.
- [7] C.C. Klepper *et al.* *Nucl. Fusion* **33** (1993) 533.
- [8] S.L. Allen *et al.*, Proc. 24 EPS Conf. on Controlled Fusion and Plasma Physics, Vol. 21A, Part III (1997) 1129.
- [9] G. Haas, *et al.*, *J. Nucl. Mater.* **121** (1984) 151.
- [10] C.C. Klepper, T.E. Evans, G. Haas, G.L. Jackson, and R. Mangi, *J. Vac. Sci. Technol. A* **11** (1993) 446.
- [11] G.L. Jackson, *et al.*, *Nucl. Fusion* **30** (1990) 2305.
- [12] M.J. Schaffer *et al.*, *Nucl. Fusion* **35** (1995) 1000.
- [13] M.R. Wade *et al.*, "Impurity Entrainment Studies Using Induced SOL Flow in DIII-D," **I-3**, this Conference.
- [14] E.A. Lazarus, *et al.*, Proc. 15th Int. Conf. on Plasma Physics and Controlled Nuclear Fusion Research, Seville, Spain, 1994, Vol. 1, p. 609 (IAEA, Vienna, 1995).
- [15] M. Greenwald, *et al.*, *Nucl. Fusion* **28** (1988) 2199.
- [16] R.L. Boivin *et al.*, *Bull. Am. Phys. Soc.* **41**(7) (1996) 1482.

ACKNOWLEDGMENTS

Work supported by U.S. DOE Contracts DE-AC05-96OR22464, W-7405-ENG-48, DE-AC03-89ER51114.